



## A novel polymer electrolyte with improved high-temperature-tolerance up to 170 °C for high-temperature lithium-ion batteries

Yan-Hua Li <sup>a,1</sup>, Xing-Long Wu <sup>a,1</sup>, Jee-Hoon Kim <sup>b</sup>, Sen Xin <sup>a</sup>, Jing Su <sup>a</sup>, Yang Yan <sup>a</sup>, Jong-Sook Lee <sup>b</sup>, Yu-Guo Guo <sup>a,b,\*</sup>

<sup>a</sup> Key Laboratory of Molecular Nanostructure and Nanotechnology, and Beijing National Laboratory for Molecular Sciences (BNLMS), Institute of Chemistry, Chinese Academy of Sciences (CAS), Beijing 100190, PR China

<sup>b</sup> School of Materials Science and Engineering, Chonnam National University (WCU), Gwangju 500-757, Republic of Korea



### HIGHLIGHTS

- Fibrous polyimide is introduced into polymer electrolyte as supporting skeleton.
- Operating temperature of polymer electrolyte has been increased up to 170 °C.
- The present polymer electrolyte exhibits outstanding high-temperature stability.
- The application range of LIBs is widened to higher temperature field above 150 °C.

### ARTICLE INFO

#### Article history:

Received 7 October 2012

Received in revised form

14 January 2013

Accepted 26 January 2013

Available online 1 February 2013

#### Keywords:

Polymer electrolyte

Ionic conductivity

High-temperature lithium-ion battery

Polyimide

Polyethylene oxide

### ABSTRACT

In this paper, a new kind of composite polymer electrolyte has been successfully prepared by casting lithium bis(oxalate)borate–succinonitrile–polyethylene oxide (LiBOB–SN–PEO) polymer electrolyte solution into porous polyimide (PI) nanofibrous films. The obtained LiBOB–SN–PEO–PI composite polymer electrolyte has been characterized by X-ray diffraction, scanning electron microscopy, differential scanning calorimetry and electrochemical impedance spectroscopy technologies in detail. It is found that the interlaced PI fibres in the framework play an important role in achieving a superior high-temperature-tolerance characteristic up to 170 °C for the LiBOB–SN–PEO–PI composite polymer electrolyte, which is much higher than that (ca. 100 °C) of traditional PEO-based electrolytes. The composite polymer electrolyte also exhibits outstanding high-temperature stability, ensuring a long-term service life in high-temperature lithium-ion batteries.

© 2013 Elsevier B.V. All rights reserved.

## 1. Introduction

Power sources are of great importance for applications in popular portable electronics, emerging electric vehicles, energy storage stations and so on. Over the last decades, rechargeable lithium-ion battery (LIB), as one of the important power sources, has been capturing considerable attention owing to its high energy density, long cycle life, and environmental friendliness [1–3]. In commercial LIBs, the electrolytes used are usually liquid solutions mainly

composed of carbonate solvents and LiPF<sub>6</sub> [4,5]. While the solvents raise the risk of explosion due to their highly volatile and flammable nature at higher temperature (>60 °C), the salt depresses the safety, the electrochemical properties and the environmental friendliness of LIBs because it could decompose thermally or hydrolyze to toxic and corrosive gases of HF and PF<sub>3</sub>O. Therefore, in the course of using LIBs, the development of advanced electrolyte with high-temperature tolerance has become more and more vital to enhance their safety and widen their applications to the high-temperature field [6–11] such as petroleum exploration, which requires the batteries working up to 200 °C [12].

Among the high-temperature electrolytes, polymer electrolyte could replace both the liquid electrolyte and the separator directly, improving the safety of LIBs. However, the melting point of commonly used polymers, such as poly(ethylene oxide) (PEO) [13], is too low to meet the practical applications of high-temperature LIBs,

\* Corresponding author. Key Laboratory of Molecular Nanostructure and Nanotechnology, and Beijing National Laboratory for Molecular Sciences (BNLMS), Institute of Chemistry, Chinese Academy of Sciences (CAS), Beijing 100190, PR China. Tel./fax: +86 10 82617069.

E-mail address: [yguo@iccas.ac.cn](mailto:yguo@iccas.ac.cn) (Y.-G. Guo).

<sup>1</sup> These authors contributed equally to this work.

because the enhanced fluidity at higher temperature may make the cathode and anode electrodes connect electronically. For example, the working temperature of widely studied PEO-based polymer electrolytes is usually limited within 100 °C due to its low melting point (66.2 °C) of PEO, although they have attracted immense interest because of their highly chemical stability, leak-proof, flexibility, low cost and high conductivity [14,15]. When the temperature goes beyond 100 °C, the fluidity of the melted polymer electrolyte makes the batteries short circuit. Compared with PEO, polyimide (PI), which is usually used as the supporting polymer material and high-performance engineering plastic due to its outstanding thermal stability and excellent mechanical strength [16], is the more proper substrate material for high-temperature polymer electrolyte.

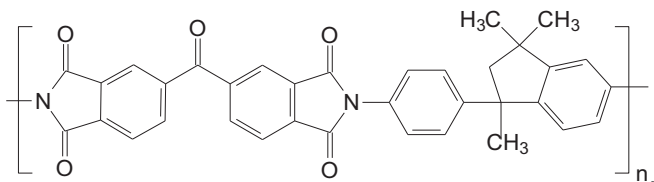
Furthermore, the thermal stabilities of traditional lithium salts (such as LiClO<sub>4</sub>, LiPF<sub>6</sub>, LiBF<sub>4</sub> and LiCF<sub>3</sub>SO<sub>3</sub>) are unsatisfactory, which further limits the increase of working temperature of polymer electrolyte. The new lithium salt, lithium bis(oxalate)borate (abbr. LiBOB, chemical formula: LiB(C<sub>2</sub>O<sub>4</sub>)<sub>2</sub>), is a very promising electrolyte for rechargeable LIBs without being corrosive toward the aluminum current collector. More importantly, it presents excellent thermal stability and chemical mildness of the decomposition products. Thermogravimetric experiments have shown that its decomposition temperature is up to 302 °C [17–19], and the decomposition products are just harmless B<sub>2</sub>O<sub>3</sub>, CO<sub>2</sub> and Li<sub>2</sub>O.

Hence, decreasing the high-temperature fluidity of polymer substrate and enhancing the thermal stability of lithium salt at the same time, may be the best way to make polymer electrolytes be workable practically and safely at high temperatures (above 100 °C). With this concept, a novel composite polymer electrolyte (CPE) with enhanced high-temperature-tolerance had been successfully prepared in the present work. The polymer electrolyte consisting of PEO and LiBOB was poured into a porous PI film prepared by the electrostatic spinning technology, which was expected to restrict the flow of the polymer electrolyte when used at high temperatures. Electrochemical test results showed that the operating temperature for the present CPE was up to 170 °C, much higher than that of traditional PEO-based polymer electrolyte (usually <80 °C).

## 2. Experimental

### 2.1. Materials

Poly(ethylene oxide) (abbr. PEO, chemical formula: (CH<sub>2</sub>CH<sub>2</sub>O)<sub>n</sub>, weight-average molecular weight: 600,000) and succinonitrile (abbr. SN, chemical formula: NCCH<sub>2</sub>CH<sub>2</sub>CN) from Aldrich were used as received. The selected polyimide (PI) was fully imidized and soluble thermoplastic polyimide, which was commercially obtained from Alfa Aesar (stock number: 43656), and its chemical structural formula was



Lithium bis(oxalate)borate (LiBOB) was prepared and purified according to the literature [20]. *N,N*-dimethylacetamide (DMAc) and acetonitrile were obtained from China Medicine Co., Ltd., and were dewatered by using 4 Å molecular sieves for at least 24 h.

### 2.2. Preparation of porous PI nanofibrous membranes

Electrospinning is an efficient method to obtain large-area porous nanofibrous membranes [21]. Here, porous PI nanofibrous membranes were prepared from 21 wt% PI solution in DMAc by electrospinning. In a typical synthesis, the electrospinning was carried out in air by using a plastic syringe with a blunt-end stainless steel needle (no. 23 needle with an inner diameter of 0.33 mm) at an applied voltage of 25 kV [22]. The feeding rate was 0.5 mL h<sup>-1</sup> and the distance from needle tip to the collector was set to be 20 cm. The products were collected by using an aluminum sheet (0.25 m in diameter) as a collector. The prepared PI nanofibrous membrane was vacuum-dried overnight at 60 °C to remove the residual solvent.

### 2.3. Preparation of polymer electrolyte

A LiBOB–SN–PEO (1:3:20 in molar ratio) solution was prepared firstly by dissolving predetermined amounts of LiBOB and SN in anhydrous acetonitrile, followed by the addition of PEO into the mixture. After the mixture became homogeneous under intense stirring for several hours, it was poured into the porous PI nanofibrous membrane and then soaked for 10 h to yield the solvent-containing composite film. To obtain the designed composite polymer electrolyte, the formed film was finally dried in a dry box at 30 °C for 24 h and successively in vacuum at 30 °C for 2 h. In a control experiment, the LiBOB–SN–PEO polymer electrolyte was prepared via a similar method [20]. In these polymer electrolytes, the added SN would play an important role on enhancing the Li<sup>+</sup> conductivity due to its effectively plastic effects [20].

### 2.4. Structural characterization of the samples

X-ray diffraction (XRD) measurements were carried out to characterize the phase purity and crystalline structure of the prepared polymer electrolytes. All the XRD patterns were collected on a Shimadzu-6000 X-ray diffractometer with Cu K $\alpha$  radiation ( $\lambda = 1.5406 \text{ \AA}$ ). The accelerating voltage was set at 40 kV with 30 mA flux at a scanning rate of 8° min<sup>-1</sup> in the 2 $\theta$  range of 10–60°. A JEOL 6701F scanning electron microscope (SEM, operating at 10 kV) was employed to investigate the morphologies of the prepared polymer electrolytes. Differential scanning calorimetry (DSC, Diamon Q100) and thermogravimetric (TG, Pyris 1 TGA, Perkin Elmer) analysis were carried out at a heating rate of 10 °C min<sup>-1</sup> in the nitrogen atmosphere to measure the thermal change and decomposition of all the polymer electrolyte membranes respectively.

### 2.5. Electrochemical characterization of the samples

The Li<sup>+</sup> conductivities of all the prepared electrolytes were measured by electrochemical impedance spectroscopy (EIS). Disk samples of polymer electrolytes were loaded in a CCR (closed-cycle-refrigerator) with a high-temperature option (CCS-450, Janis, USA) in vacuum. The Ag paste (colloidal silver paste, Ted Pella, USA) was used as electrodes for electrical measurements. The impedance spectra were obtained using an FRA analyzer (Solartron 1260, Ametek, UK) combined with a high dielectric interface (Solartron 1296, Ametek, UK) over the frequency range between 1 MHz and 1 Hz at the amplitude of 10 mV from 0 to 170 °C. Before the collections of each EIS spectrum, the assembled cells were firstly placed at the given temperature for 2 h. Linear sweep voltammetry (LSV) experiments were performed to investigate the electrochemical stability of the samples using a three electrode cell with stainless steel working electrode and lithium reference and counter

electrodes. All experiments were carried out at a sweep rate of  $10 \text{ mV s}^{-1}$  in the voltage range of 0–7 V (vs.  $\text{Li}^+/\text{Li}$ ) at 25 °C.

### 3. Results and discussion

#### 3.1. Structural characterization

With the electrospinning technology, a large-area yellow PI film has indeed been obtained. It could be patterned into required sizes and shapes. Fig. 1a is the photograph of one punched circular slice with a diameter of about 72 mm. Its microstructures are further characterized by SEM. As shown in Fig. 1b, the PI films are composed of uniform nanofibres with an average diameter of about 900 nm and lengths of hundreds of micrometer. The nanofibres are interlaced and overlapped randomly each other, forming many interspaces and pores of about several micrometers, which could be filled in by the following poured LiBOB–SN–PEO polymer electrolyte solution. Fig. 1c and d is the surface and cross-section SEM images of obtained composite polymer electrolyte. As shown in Fig. 1c, its surface is very smooth and homogeneous with only few ripples on it. The thickness of the film is about 110  $\mu\text{m}$  (Fig. 1d), which is equal to the unfilled porous PI films. No interspaces and pores are observed in either surface or cross-section, demonstrating the complete infiltration of PEO-based electrolyte into the porous PI substrate, and a novel LiBOB–SN–PEO–PI CPE with a novel structure has formed. In the composite, the interlaced and continuous PI nanofibres act as a robust skeleton, which could effectively restrict the flow of LiBOB–SN–PEO polymer electrolyte when worked at elevated temperature. That guarantees the high-temperature workability for LiBOB–SN–PEO–PI CPE compared with pristine LiBOB–SN–PEO polymer electrolyte, as demonstrated in the part of electrochemical tests.

Fig. 2 shows the XRD patterns of porous PI film, LiBOB–SN–PEO electrolyte and the obtained LiBOB–SN–PEO–PI CPE. In the XRD pattern of porous PI film, only weak diffraction hump in the  $2\theta$  range of 10°–35° is observed, indicating the amorphous nature of

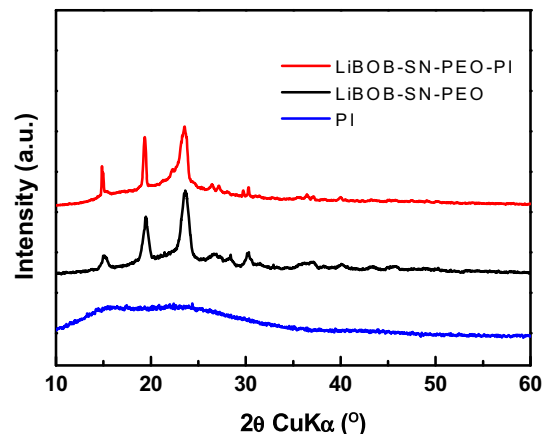


Fig. 2. XRD patterns of porous PI film, LiBOB–SN–PEO electrolyte and LiBOB–SN–PEO–PI composite polymer electrolyte.

the PI substrate. The diffraction peaks of the other two XRD patterns are almost the same, demonstrating that the LiBOB–SN–PEO electrolyte has been poured successfully into the porous PI substrate, which is in good agreement with the SEM observation (Fig. 1c and d). In addition, it also indicates that the addition of PI skeleton does not lead to more crystalline of the polymer electrolyte, which is good for high  $\text{Li}^+$  conductivity.

Fig. 3 summarizes the DSC thermograms and TG curves of the porous PI film, the LiBOB–SN–PEO electrolyte and the obtained LiBOB–SN–PEO–PI composite polymer electrolyte. As shown in Fig. 3a, there is no endothermic–exothermic process for structure reforming for the pure PI film, revealing its outstanding thermal stability in the whole temperature range from –50 °C to 200 °C. This result implies that PI is a favorable skeleton to restrict the high-temperature flow of the polymer electrolyte and improve its high-temperature performance. For the two electrolytes, the DSC profile of the LiBOB–SN–PEO–PI composite polymer electrolyte is

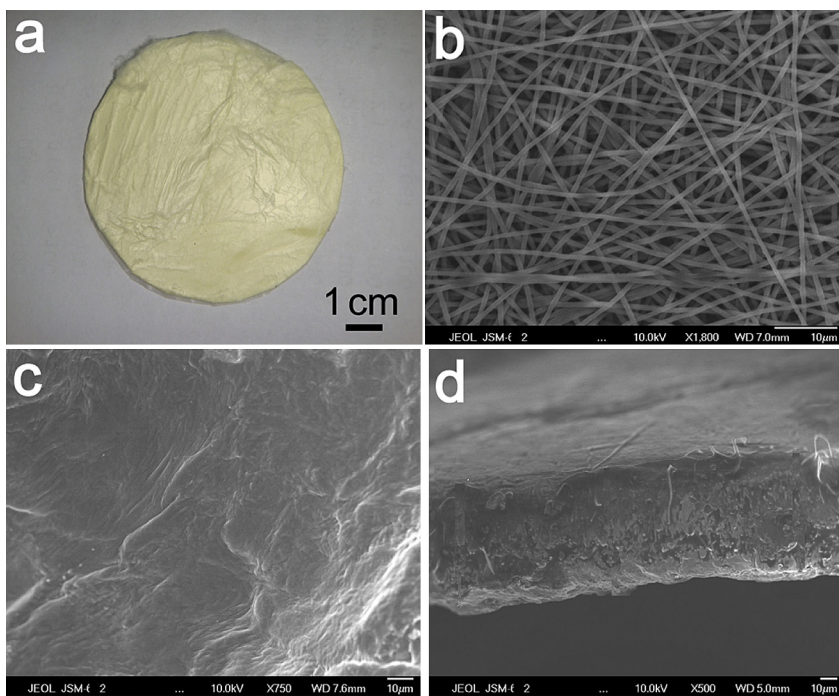


Fig. 1. Photograph (a) and SEM image (b) of porous PI nanofibrous film prepared by electrospinning technology; SEM images showing the surface (c) and the cross-section (d) of the prepared LiBOB–SN–PEO–PI composite polymer electrolyte.

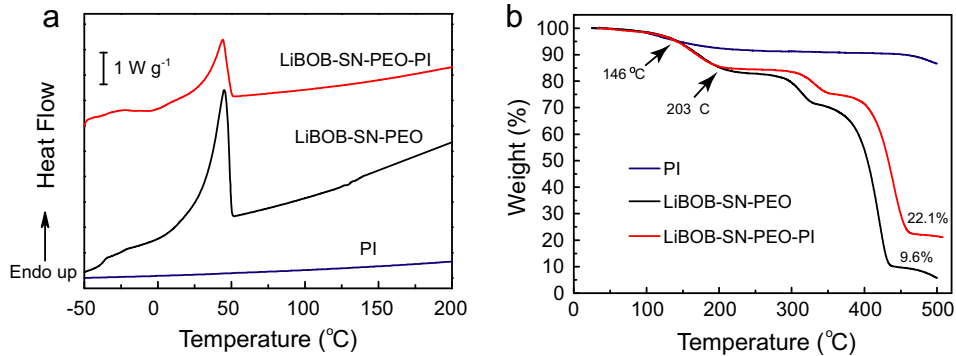


Fig. 3. DSC thermograms (a) and thermogravimetric curves (b) of porous PI film, LiBOB-SN-PEO electrolyte and LiBOB-SN-PEO-PI composite polymer electrolyte.

almost the same as that of the LiBOB-SN-PEO electrolyte except for lower endothermal value above 120 °C, and their crystalline melting temperatures ( $T_m$ , about 47 °C) are equal. These results further confirm that the pores of PI substrate have been filled in by the LiBOB-SN-PEO electrolyte without chemical reaction occurring between them and the formation of new chemicals, which is consistent with the SEM and XRD characterization results. The values of heat enthalpy ( $\Delta H_m$ ) to the crystalline melting process are 53.3 J g<sup>-1</sup> and 46.5 J g<sup>-1</sup> for LiBOB-SN-PEO and LiBOB-SN-PEO-PI respectively. The lower  $\Delta H_m$  value for LiBOB-SN-PEO-PI may be simply attributed to existence of the no endothermic-exothermic PI skeleton in the CPE. It could be roughly calculated that the mass ratio of PI in LiBOB-SN-PEO-PI CPE is about 12.8% (=1–46.5 J g<sup>-1</sup>/53.3 J g<sup>-1</sup>), which is consistent with the TG test result (Fig. 3b, 12.5% = 22.1%–9.6%). Furthermore, as DSC thermograms and TG curves shown in Fig. 3, the LiBOB-SN-PEO-PI CPE exhibits an improved high-temperature tolerance and stability compared to the pristine LiBOB-SN-PEO polymer electrolyte, because of the introduction of interlaced PI nanofibres as skeleton. Firstly, the LiBOB-SN-PEO-PI CPE displays much flatter DSC curve than LiBOB-SN-PEO between 100 and 200 °C, i.e., the endothermal value of the former is much lower than that of the latter, although both exhibit the same thermal stability below about 200 °C in TG curves. Secondly, the LiBOB-SN-PEO-PI CPE reveals higher thermal decomposition temperature than LiBOB-SN-PEO above 200 °C (Fig. 3b).

### 3.2. Electrochemical characterization

The Li<sup>+</sup> conductivities of all the polymer electrolytes are investigated via EIS method. The characteristic EIS responses at different

temperatures are presented in Fig. 4. At the lower temperature, the Nyquist plot consists of a depressed circle at high frequencies followed by a slanted line at low frequencies as shown in Fig. 4a. As the temperature increases, the resistance of the film becomes much lower and thus the relaxation time of the high-frequency response becomes shorter so either the high-frequency circular response goes out of the experimental frequency range or is replaced by the inductive response below the real axis. In addition, the transition temperature of two different kinds of Nyquist plots is about 110 °C. It is worth noting that the prepared LiBOB-SN-PEO-PI composite polymer electrolyte can work at a very high temperature of up to 170 °C without any short circuit.

To obtain the Li<sup>+</sup> conductivities ( $\sigma$ ), two different equivalent circuits are used to fit the different Cole–Cole plots respectively, as shown in the corresponding insets of Fig. 4, where the black lines are experimental data of EIS responses and the red lines are the fitted results. In the equivalent circuits,  $R_b$  is the bulk ionic resistance of the polymer electrolytes,  $Q_{dl}$  is the constant phase element of the interfacial double layer contributing to the slanted lines in the plots, and  $Q_g$  is the geometric capacitance. The EIS test results are fitted well using the suggested equivalent circuits. According to the equation,  $\sigma = L/(R_b A)$ , where  $L$  and  $A$  are the thickness and area of polymer electrolyte electrodes respectively, and  $R_b$  can be obtained from fitted results of EIS, the  $\sigma$  values can be easily and accurately calculated.

Fig. 5 presents the variation of  $\sigma$  values of the prepared LiBOB-SN-PEO-PI composite polymer electrolytes and LiBOB-SN-PEO electrolyte along with operating temperature. It has been reported that the maximum working temperature for PEO-based polymer electrolytes is usually about 80 °C. If the working temperature

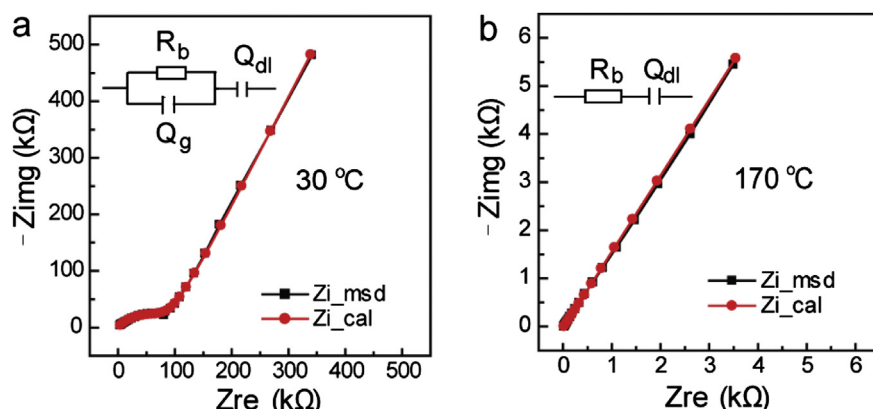
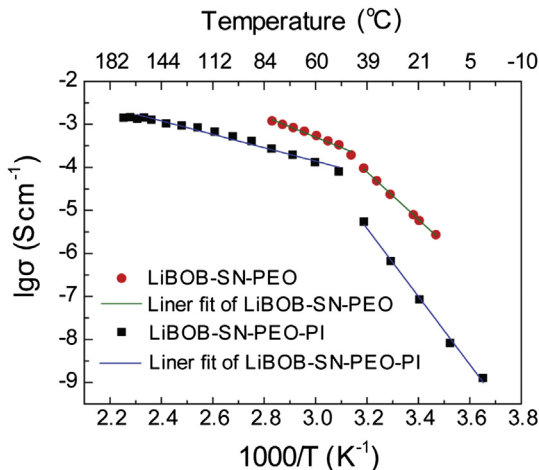


Fig. 4. The typical Nyquist plots of EIS measurements of the obtained PEO-LiBOB-SN-PI composite polymer electrolyte at (a) 30 °C and (b) 170 °C. The insets in both figures are the corresponding equivalent circuits for fitting the EIS responses. The black lines show the experimental data and the red lines show the fitted results. (For interpretation of the references to color in this figure legend, the reader is referred to the web version of this article.)



**Fig. 5.** Arrhenius plots of temperature dependent  $\lg \sigma$  of LiBOB–SN–PEO–PI composite polymer electrolytes and LiBOB–SN–PEO electrolyte. The black squares and red circles are the experimental results and the lines are the liner fitted results. (For interpretation of the references to color in this figure legend, the reader is referred to the web version of this article.)

is higher than 80 °C, its fluidity increases, which may lead to the destroyed short circuit. Therefore, the  $\sigma$  values of LiBOB–SN–PEO electrolyte above 80 °C cannot be tested, as shown in Fig. 5. Excitingly, after the introduction of PI nanofibres into LiBOB–SN–PEO electrolyte as the structural support, the working temperature increases remarkably to 170 °C. As shown in Fig. 5, the  $\sigma$  value of the LiBOB–SN–PEO–PI composite polymer electrolyte also remains at  $1.46 \times 10^{-3}$  S cm<sup>-1</sup> at the high working temperature of 170 °C. The conductivity of the LiBOB–SN–PEO–PI CPE is lower than that of the pristine LiBOB–SN–PEO polymer electrolyte at the low temperature range (<80 °C), which could be attributed to the PI skeleton in the LiBOB–SN–PEO–PI CPE. On the surface of the LiBOB–SN–PEO–PI CPE, there usually exist some PI nanofibers, which especially reduce the real contact area between CPE and current corrector, i.e. the real contact area ( $A_r$ ) for  $\text{Li}^+$  conductivity is noticeably smaller than the used geometric area ( $A_u$ ) for  $\sigma$  calculation. Therefore, the obtained  $\sigma$  value of the LiBOB–SN–PEO–PI CPE is smaller than the pure LiBOB–SN–PEO polymer electrolyte at low temperature, according to the equation  $\sigma = L/(R_b A)$ . Note that the melting PEO could release this effect at high temperature.

Additionally, It can be clearly seen from Fig. 5 that both the two plots display an inflection point at about 50 °C, which is similar to most of the PEO-based CPEs reported [23]. The inflection points may be related to the transition of PEO from crystalline phase to the amorphous one. To compare the differences of  $\text{Li}^+$  transformation behaviors between crystalline and amorphous phase, their  $\sigma$  values are fitted by Arrhenius formula respectively, i.e.,

$$\sigma = \sigma_0 \exp\left(\frac{-E_a}{RT}\right)$$

where  $\sigma_0$  is the pre-exponential factor;  $E_a$  is the pseudo activation energy for ionic transport;  $R$  is the gas constant and  $T$  is the test absolute temperature. As shown in Fig. 5, the experimental data have been fitted well by Arrhenius formula with all the correlation coefficients higher than 98%. To analyze and discuss the processes of  $\text{Li}^+$  migration deeply, the  $E_a$  is first evaluated by the slope of the fitted line below or above the inflection point, and the corresponding values are collected in Table 1, because it is relevant and crucial to the conductivity enhancement for composite polymer electrolyte. When temperature is below 50 °C, both the LiBOB–SN–

**Table 1**

Activation energies of LiBOB–SN–PEO polymer electrolyte and LiBOB–SN–PEO–PI polymer electrolyte, among which  $E_{a1}$  represents the activation energy in temperature range lower than the inflection temperature, while  $E_{a2}$  represents the activation energy in temperature range higher than the inflection temperature.

Samples	$E_{a1}$ (kJ mol <sup>-1</sup> )	$E_{a2}$ (kJ mol <sup>-1</sup> )
LiBOB–SN–PEO	19.80	8.71
LiBOB–SN–PEO–PI	28.44	5.62

PEO and LiBOB–SN–PEO–PI composite polymer electrolytes are in high degree of crystallization, so the  $\text{Li}^+$  conductivities are low due to the large activation energies (19.80 kJ mol<sup>-1</sup> for LiBOB–SN–PEO and 28.44 kJ mol<sup>-1</sup> for LiBOB–SN–PEO–PI composite polymer electrolyte as shown in Table 1) for  $\text{Li}^+$  conduction. At the inflection point of about 50 °C, both the  $\text{Li}^+$  conductivities increase abruptly (Fig. 5) because of the transition of composite polymer electrolyte from crystalline phase to amorphous one, which is consistent with the DSC test results. In the temperature range above the inflection point, corresponding to the amorphous state of composite polymer electrolyte, the  $E_a$  values of the LiBOB–SN–PEO and LiBOB–SN–PEO–PI composite polymer electrolytes decrease to 8.71 kJ mol<sup>-1</sup> and 5.62 kJ mol<sup>-1</sup>, respectively. The lower the activation energy, the easier the  $\text{Li}^+$  conduction. Therefore, the  $\text{Li}^+$  transmitting capability of both the composite polymer electrolytes is markedly enhanced at the amorphous state in comparison with the crystalline phase. Furthermore, compared with the pristine LiBOB–SN–PEO composite polymer electrolyte, the present PI-supported LiBOB–SN–PEO–PI exhibits much better  $\text{Li}^+$  transmitting capability, which may be resulted from its novel and self-supporting structure.

For one high-temperature polymer electrolyte, its high-temperature stability is an important factor for practical application. Therefore, we have investigated the high temperature (150 °C) stability of the prepared LiBOB–SN–PEO–PI composite polymer electrolyte by conductivity monitoring. As shown in Fig. 6, the  $\sigma$  is always stable at around  $1.23 \times 10^{-3}$  S cm<sup>-1</sup> for 120 h (about 5 days), which ensures the long-term application at the corresponding temperature. Furthermore, the electrochemical stability of the LiBOB–SN–PEO–PI CPE was also investigated by LSV experiments. As shown in Fig. 7, the stable electrochemical window of LiBOB–SN–PEO–PI CPE is 0.32–5.35 V (vs.  $\text{Li}^+/\text{Li}$ ), which is adequate for LIB working, although it is slightly narrower than the pure LiBOB–SN–PEO electrolyte (0.18–5.6 V vs.  $\text{Li}^+/\text{Li}$ ). In addition, the LiBOB–SN–PEO–PI composite polymer electrolyte is flexible and self-standing, implying its high-temperature application in LIBs free of any separator.

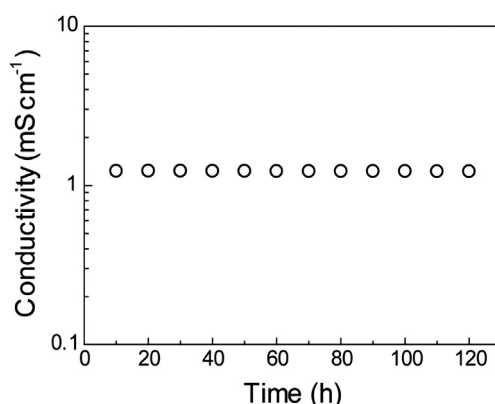


**Fig. 6.** LiBOB–SN–PEO–PI composite polymer electrolyte conductivity vs. time at 150 °C.

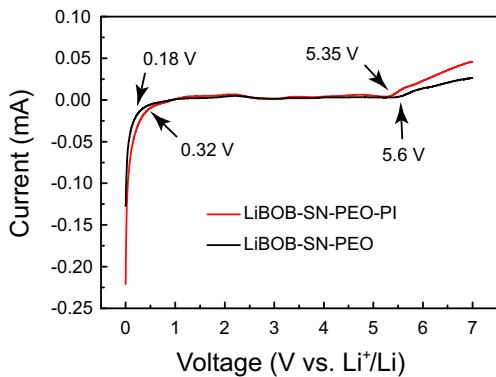


**Fig. 7.** Linear sweep voltammograms of LiBOB–SN–PEO–PI composite polymer electrolytes and LiBOB–SN–PEO electrolyte at a sweep rate of  $10 \text{ mV s}^{-1}$ .

#### 4. Conclusions

One novel LiBOB–SN–PEO–PI composite polymer electrolyte was prepared through a facile solution method and was characterized by XRD, DSC, SEM and EIS technologies. All the data reported in this work confirm the unique role of the PI nanofibrous film as a fine supporting material in increasing the working temperature of the PEO-based polymer electrolyte. Porous PI nanofibrous film supported polymer electrolyte can be operated at  $170^\circ\text{C}$  with superior  $\text{Li}^+$  conduction. In addition, the prepared LiBOB–SN–PEO–PI composite polymer electrolyte is flexible and self-standing with good mechanical properties, implying its use in LIBs without any commercial separator. These features make the LiBOB–SN–PEO–PI composite polymer electrolyte a promising electrolyte to develop advanced, high-performance lithium polymer rechargeable batteries operating at high temperatures ( $140$ – $170^\circ\text{C}$ ).

#### Acknowledgments

This work was supported by the National Natural Science Foundation of China (Nos. 21073205 and 51225204), the National

Key Project on Basic Research (No. 2011CB935700), and the WCU program through NRF funded by MEST (R32-2009-000-20074-0). X.L.W. gratefully acknowledges the support of K.C. Wong Education Foundation.

#### References

- [1] J. Maier, *Nat. Mater.* 4 (2005) 805–815.
- [2] L.Z. Fan, T. Xing, R. Awan, W. Qiu, *Ionics* 17 (2011) 491–494.
- [3] Y.G. Guo, J.S. Hu, L.J. Wan, *Adv. Mater.* 20 (2008) 2878–2887.
- [4] Z.H. Li, Q.L. Xia, L.L. Liu, G.T. Lei, Q.Z. Xiao, D.S. Gao, X.D. Zhou, *Electrochim. Acta* 56 (2010) 804–809.
- [5] J.M. Tarascon, M. Armand, *Nature* 414 (2001) 359–367.
- [6] F. Mestre-Aizpurua, S. Laruelle, S. Gruegeon, J.M. Tarascon, M.R. Palacin, *J. Appl. Electrochem.* 40 (2010) 1365–1370.
- [7] F. Mestre-Aizpurua, S. Hamelet, C. Masquelier, M.R. Palacin, *J. Power Sources* 195 (2010) 6897–6901.
- [8] C.K. Park, A. Kakirde, W. Ebner, V. Manivannan, C. Chai, D.J. Ihm, Y.J. Shim, *J. Power Sources* 97–8 (2001) 775–778.
- [9] Q.C. Hu, S. Osswald, R. Daniel, Y. Zhu, S. Wesel, L. Ortiz, D.R. Sadoway, *J. Power Sources* 196 (2011) 5604–5610.
- [10] L.P. Mao, B.C. Li, X.L. Cui, Y.Y. Zhao, X.L. Xu, X.M. Shi, S.Y. Li, F.Q. Li, *Electrochim. Acta* 79 (2012) 197–201.
- [11] H.H. Zheng, Q.T. Qu, L. Zhang, G. Liu, V.S. Battaglia, *RSC Adv.* 2 (2012) 4904–4912.
- [12] M.R. David, J.B. Leriche, C. Delacourt, P. Poizot, M.R. Palacin, J.M. Tarascon, *Electrochim. Commun.* 9 (2007) 708–712.
- [13] A.J. Bhattacharyya, J. Fleig, Y.G. Guo, J. Maier, *Adv. Mater.* 17 (2005) 2630–2634.
- [14] F. Croce, S. Sacchetti, B. Scrosati, *J. Power Sources* 162 (2006) 685–689.
- [15] J.R. Kim, S.W. Choi, S.M. Jo, W.S. Lee, B.C. Kim, *Electrochim. Acta* 50 (2004) 69–75.
- [16] Y.Y. Lv, J. Wu, L.S. Wan, Z.K. Xu, *J. Phys. Chem. C* 112 (2008) 10609–10615.
- [17] D. Chen, R. Wang, W.W. Tjiu, T. Liu, *Comp. Sci. Technol.* 71 (2011) 1556–1562.
- [18] K. Xu, S. Zhang, T.R. Jow, W. Xu, C.A. Angell, *Electrochim. Solid-State Lett.* 5 (2002) A26.
- [19] S. Wang, W. Qiu, Y. Guan, B. Yu, H. Zhao, W. Liu, *Electrochim. Acta* 52 (2007) 4907–4910.
- [20] X.L. Wu, S. Xin, H.H. Seo, J. Kim, Y.G. Guo, J.S. Lee, *Solid State Ionics* 186 (2011) 1–6.
- [21] D. Chen, T.X. Liu, X.P. Zhou, W.C. Tjiu, H.Q. Hou, *J. Phys. Chem. B* 113 (2009) 9741–9748.
- [22] P. Tsai, H. Schreudergibson, P. Gibson, *J. Electrostat.* 50 (2002) 333–341.
- [23] Z. Tang, J. Wang, Q. Chen, W. He, C. Shen, X.-X. Mao, J. Zhang, *Electrochim. Acta* 52 (2007) 6638–6643.